

# RESPIRATORY AIRFLOW ESTIMATION FROM LUNG SOUNDS BASED ON REGRESSION

Elmar Messner<sup>1</sup>, Martin Hagmüller<sup>1</sup>, Paul Swatek<sup>2</sup>, Freyja-Maria Smolle-Jüttner<sup>2</sup>, and Franz Pernkopf<sup>1</sup>

<sup>1</sup>Signal Processing and Speech Communication Laboratory  
Graz University of Technology, Austria

<sup>2</sup>Division of Thoracic and Hyperbaric Surgery  
Medical University of Graz, Austria

## ABSTRACT

The aim of this work is the estimation of respiratory flow from lung sound recordings, i.e. acoustic airflow estimation. With a 16-channel lung sound recording device, we simultaneously record the respiratory flow and the lung sounds on the posterior chest from six lung-healthy subjects in supine position. For the recordings of four selected sensor positions, we extract linear frequency cepstral coefficient (LFCC) features and map these on the airflow signal. We use multivariate polynomial regression to fit the features to the airflow signal. Compared to most of the previous approaches, the proposed method uses lung sounds instead of trachea sounds. Furthermore, our method masters the estimation of the airflow without prior knowledge of the respiratory phase, i.e. no additional algorithm for phase detection is required. Another benefit is the avoidance of time-consuming calibration. In experiments, we evaluate the proposed method for various selections of sensor positions in terms of mean squared error (MSE) between estimated and actual airflow. Moreover, we show the accuracy of the method regarding a frame-based breathing-phase detection.

**Index Terms**— lung sounds, multichannel recording device, acoustic airflow estimation, linear frequency cepstral coefficients (LFCCs), multivariate polynomial regression

## 1. INTRODUCTION

In lung sound research, the simultaneous measurement of airflow in addition to the lung sounds is essential. First of all, the airflow signal enables the distinction between inspiratory and expiratory phases. Furthermore, it provides information about the current state of the lung. The real-time airflow feedback for the subject further supports a controlled measurement procedure. The most common device for airflow measurement is the spirometer, which is suitable for short-time airflow measurements, but not for continuous airflow monitoring. Alternatives, like nasal cannula and/or resistance bands, enable a continuous airflow monitoring, but are not as accurate [1]. Therefore, acoustic airflow estimation (AAE) facilitates the short-time recording of lung sounds by making the spirometer needless, and it can be an accurate alternative for continuous airflow monitoring.

In most of the existing approaches, the acoustic airflow estimation is considered as a twofold task: the breathing phase detection

---

This project was supported by the government of Styria, Austria, under the project call HTI:Tech\_for\_Med and by the Austrian Science Fund (FWF) under the project number P27803-N15. The authors acknowledge 3M™ for providing Littmann® stethoscope chest pieces and Schiller AG for the support with a spirometry solution.

(BPD) and the airflow estimation. For the BPD the difference of lung sound intensity between inspiratory and expiratory phase can be used [2]. Due to the direct correlation of trachea sounds and airflow, most of the previous approaches for AAE are based on trachea sounds instead of lung sounds [1, 3, 4, 5]. For the existing approaches, we observe the following limitations: a need for calibration, no multichannel information is used (only based on single channel trachea/lung sound recording) and heart sound interference is partially ignored.

Based on the afore mentioned limitations, our motivation is to find a single model for AAE, without the need for an additional BPD-algorithm. Furthermore, we are interested in a calibration free approach. Therefore, we recorded lung sounds in supine position on the posterior chest of six subjects at several airflow rates with our previously developed 16-channel lung sound recording device [6]. For the lung sound recordings, we extract LFCC-features and map these to the corresponding airflow signal. We use multivariate polynomial regression analysis to fit the features to the airflow signal for the recordings of the subjects. In experiments, we investigate several sensor selections (sensor sets), which differ in number and position. Furthermore, we examine the impact of heart sounds on the accuracy. We investigate also the performance of the proposed method for BPD.

We organized the paper as follows: Section 2 describes the data acquisition, the recording material and the acoustic airflow estimation model. In Section 3, we show experimental results, which we further discuss in Section 4. Section 5 concludes the paper.

## 2. METHOD

### 2.1. Data Acquisition

For the recordings, we used a multichannel lung sound recording device, which includes the feature of simultaneous airflow recording [6]. It consists of a multichannel lung sound recording front-end (see Figure 1) and a pneumothachograph.

The multichannel lung sound recording front-end is a foam pad with a cover of artificial leather, a similar construction as the Stethographics STG 16 [7]. We arranged 16 lung sound transducers (LSTs) on the topmost layer of the pad with a fixed pattern, which is comparable to the one proposed in [8]. For the LST-design, we applied the approach with air-coupled electret-condenser microphones [9]. Therefore, we modified a Littmann Classic II chest piece. The foam pad enables the recording of lung sounds in the supine position, performed on an examination table with the pad placed under the back of the patient.

For the analogue pre-filtering, pre-amplification, and digitization of the LST signals, we use standard audio recording equipment.

The sampling frequency for the lung sound signals is  $f_s = 16$  kHz and the resolution is 24 bit. Before analog-to-digital conversion, we filter the LST-signal with a Bessel high-pass filter with a cut-off frequency of  $f_c = 80$  Hz and a slope of 24 dB/oct.

The pneumotachograph is a Schiller SP 260, which is connected via the USB port. The sampling frequency for the airflow signal is  $f_s = 400$  Hz.

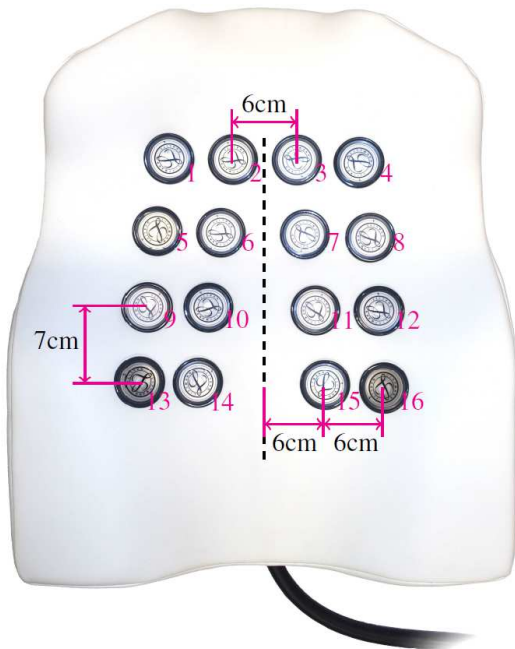


**Fig. 1.** Multichannel recording front-end of the lung sound recording device [6]. 16 lung sound transducers are distributed on the foam pad. The center line represents the spine.

To calibrate the recording device, we used a Brüel & Kjær sound calibrator Type 4231. We adjusted the microphone preamplifiers of the LSTs to reach the same signal level for the sound calibrator signal (sinusoidal waveform with a frequency of  $f = 1$  kHz and a sound pressure level of 94 dB).

## 2.2. Subjects and Materials

We recorded lung sounds over the posterior chest of six lung-healthy subjects at airflow rates of 0.3, 0.7, 1.0, 1.3 and 1.7 l/s. During the recording the subjects wore a nose clip and held the pneumotachograph with both hands. We instructed the subjects to breath steadily during inspiration at the given airflow rates, with natural breathing during expiration, by providing a real-time feedback for the airflow rate. For the orientation of the subject on the pad, we used a defined distance  $d \approx 7$  cm between the 7th cervical vertebra ( $C_7$ ) and the center line of the topmost row of sensors. For each subject, we have 16-channel lung sound recordings at five different airflow rates, with 3-8 breathing cycles within 30 seconds, respectively. The subjects were six male volunteers, with no diagnosed lung diseases. The average age of the subjects was  $27 \pm 1$  years, the weight  $76 \pm 2$  kg, the height  $180 \pm 7$  cm and the body mass index  $24 \pm 2$ . Figure 2 shows examples of phonopneumograms (overlapping illustration of lung sounds and airflow signals) for one subject, recorded with

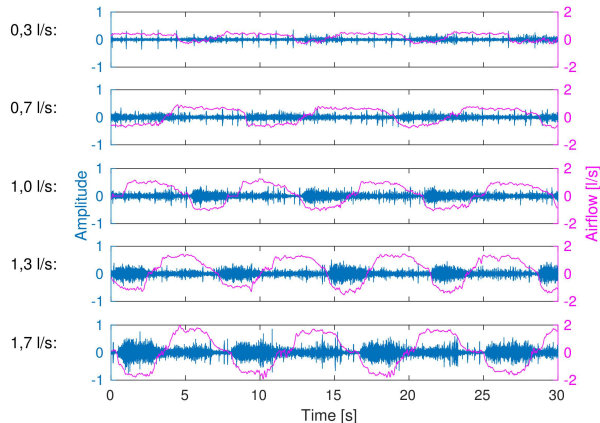


**Fig. 2.** Phonopneumograms of sensor 12 from one subject for different maximum inspiratory airflow values (0.3, 0.7, 1.0, 1.3 and 1.7 l/s). Legend: — Lung Sound Recording; — Airflow of Pneumotachograph

sensor 12. For the experiments in Section 3.2, we manually labeled the sections of the lung sound recordings contaminated with heart sounds.

## 2.3. Acoustic Airflow Estimation based on Regression

For the lung sound recordings, we extract LFCC-features and map these to the airflow signal. We compute the LFCC-features by framing the lung sound signal of each sensor with a duration of  $T_w = 25$  ms and a 75 % overlap between adjacent frames. We multiply each frame with a Hamming window. The number of filter bank channels is  $M = 5$ . For each frame, we compute four cepstral coefficient  $C = 4$ . The feature vector for multivariate polynomial regression is obtained by stacking the cepstral coefficients of the selected sensors. We map each vector to the value of the corresponding down-sampled airflow signal (new sampling frequency  $f_{s,new} = 160$  Hz). We use multivariate polynomial regression analysis to find a 3<sup>rd</sup> order polynomial fit between the features and the airflow signal. We include the cross-terms in the regression model. To smooth the output of the regression model, we use a low-pass filter with a cut-off frequency  $f_c = 3$  Hz.

## 3. RESULTS

### 3.1. Acoustic Airflow Estimation

Our acoustic airflow estimation approach is based on the spectral information of the locally varying lung sounds, i.e. lung sounds differ for each sensor position. Therefore, we use bronchial and vesicular lung sounds. We record bronchial lung sounds over the large airways approximately at the 3<sup>rd</sup> intercostal space (Sensors 2 and 3). The vesicular lung sound is recorded over the lung periphery approximately at the 8<sup>th</sup> intercostal space (Sensor 9 and 12). For the experiments within this section, we consider a frequency band with a lower cut-off frequency  $f_L = 100$  Hz and an upper cut-off frequency  $f_H = 1000$  Hz, i.e. we extract the LFCCs, as described in Section 2.3, for this frequency band.

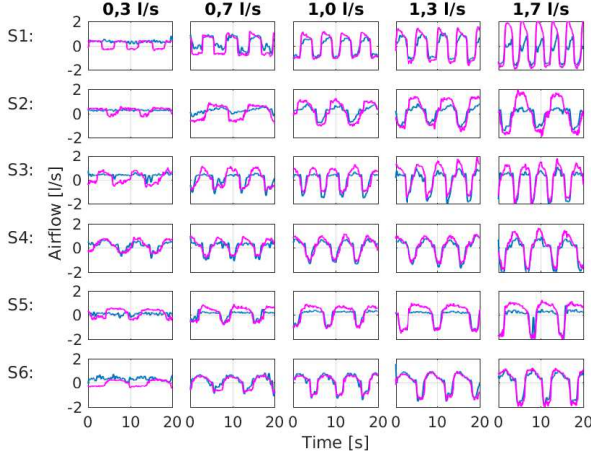
### 3.1.1. Selection of Sensors with Leave-One-Out Cross-Validation

Table 1 shows the results in terms of MSE between estimated and actual airflow for different sets of sensors (cf. Figure 1). We report results separately for different recordings from shallow to deep breathing (maximum inspiratory airflow values from 0.3 to 1.7 l/s). Therefore, we perform leave-one-out cross-validation with the recordings of five subjects for training, and the recordings of the remaining subject for evaluation. The training material consists of 10 seconds from

Sensors	Maximum Inspiratory Airflow Value				
	0.3 l/s	0.7 l/s	1.0 l/s	1.3 l/s	1.7 l/s
{2,3}	0.16±0.22	0.19±0.24	0.20±0.26	0.35±0.56	0.63±1.23
{9,12}	0.17±0.22	0.17±0.23	0.13±0.19	0.21±0.34	0.45±0.97
{2,9}	0.15±0.20	0.18±0.26	0.11±0.14	0.17±0.25	0.31±0.52
{3,12}	0.16±0.22	0.16±0.23	0.15±0.23	0.22±0.42	0.55±1.37
{2,3,9,12}	0.14±0.19	0.14±0.16	0.11±0.14	0.17±0.27	0.43±0.95

**Table 1.** Acoustic airflow estimation for different sensor combinations between shallow and deep breathing. The MSE between estimated and actual airflow is reported.

each of the recordings at the different airflow rates for each subject. This duration covers at least one full breathing cycle. The material for evaluation consists of 20 seconds, respectively. The results for sensor set {2,3,9,12} are illustrated in Figure 3 for all test subjects (S1-S6) independently.



**Fig. 3.** Acoustically estimated and actual airflow waveforms for all test subjects (S1-S6) between shallow and deep breathing (0.3 – 1.7 l/s). The selected sensor set is {2,3,9,12}. Legend: — Airflow of Pneumotachograph; — Acoustic Airflow Estimation

### 3.1.2. Single Subject for Training and Evaluation

In this section, we investigate the performance of the AAE method performing training and testing on data of the same subject. We use 10 seconds of the recorded material from one subject for training and the remaining 20 seconds for evaluation. The selected set of sensors is {2,3,9,12}. Table 2 shows the results in terms of MSE between estimated and actual airflow for each of the subjects independently.

Subject	Maximum Inspiratory Airflow Value				
	0.3 l/s	0.7 l/s	1.0 l/s	1.3 l/s	1.7 l/s
S1	0.37±1.6	0.12±0.16	0.06±0.18	0.05±0.07	0.06±0.08
S2	0.08±0.12	0.15±0.19	0.08±0.12	0.14±0.19	0.24±0.35
S3	0.21±0.29	0.04±0.06	0.04±0.06	0.06±0.11	0.05±0.07
S4	0.07±0.09	0.04±0.07	0.03±0.07	0.05±0.09	0.09±0.10
S5	0.07±0.10	0.04±0.08	0.03±0.07	0.02±0.04	0.12±0.14
S6	0.12±0.16	0.03±0.07	0.02±0.06	0.02±0.06	0.07±0.15

**Table 2.** Acoustic airflow estimation performing training and testing on data of the same subject. The MSE between estimated and actual airflow is reported.

### 3.1.3. Effect of Heart Sounds

Within this section, we investigate the influence of heart sounds on the regression performance. Our recording setup includes an analogue high-pass filter with a cut-off frequency of  $f_c = 80$  Hz (cf. Section 2.1) to filter out low frequency noise. However, heart sounds are still contaminating the lung sound recordings in the lower frequency range, mainly up to a frequency of  $f \approx 200$  Hz [10]. Therefore, we compared three setups, differing either in the considered bandwidth or the presence of heart sounds:

- Setup 1: Basic setup, where we consider the frequency band between 100 and 1000 Hz, as in the previous sections.
- Setup 2: We consider the heart sound free frequency range between 400 and 1000 Hz, i.e. we extract the LFCCs, as described in Section 2.3, for this frequency band.
- Setup 3: As Setup 1, but we use only frames free from heart sounds (cf. Section 2.2) for training and evaluation.

For the experiments, we use the recordings of one subject (S2). For each setup, we use 1600 frames (corresponds to 10 seconds of the recordings) for training and 1600 independent frames for testing, for each of the recordings at different airflow rates. The selected set of sensors is {2,3,9,12}. For the experiments within this section, we do not smooth the output of the regression model. In Table 3, we show the results for the three setups for the different maximum inspiratory airflow rates.

Setup	Maximum Inspiratory Airflow Value				
	0.3 l/s	0.7 l/s	1.0 l/s	1.3 l/s	1.7 l/s
1	0.10±0.18	0.24±0.36	0.18±0.44	0.28±0.61	0.39±0.70
2	0.09±0.18	0.24±0.43	0.17±0.38	0.36±0.88	0.48±0.85
3	0.10±0.17	0.18±0.31	0.19±0.55	0.23±0.56	0.37±0.76

**Table 3.** Influence of heart sounds on acoustic airflow estimation. We compare the results for three different setups. The MSE between estimated and actual airflow is reported.

## 3.2. Breathing Phase Detection

We investigate the performance of the proposed method regarding a frame-based breathing phase detection, i.e. the distinction between inspiratory and expiratory phase. Table 4 shows the experimental results by means of sensitivity, specificity and accuracy. The sensitivity measures the proportion of frames that are correctly identified as expiratory phase, i.e. positiv airflow values. The specificity

measures the proportion of frames that are correctly identified as inspiratory phase, i.e. negative airflow values. Figure 4 illustrates the correct (blue area) and incorrect (red area) breathing phase detection. The setup is the same as the one described in Section 3.1.1 with the sensor set {2,3,9,12}.

Measures	Maximum Inspiratory Airflow Value				
	0.3 l/s	0.7 l/s	1.0 l/s	1.3 l/s	1.7 l/s
Sensitivity (%)	13	68	86	89	91
Specificity (%)	97	98	98	98	90
Accuracy (%)	63	88	93	95	91

**Table 4.** Breathing phase detection from shallow to deep breathing in [%].

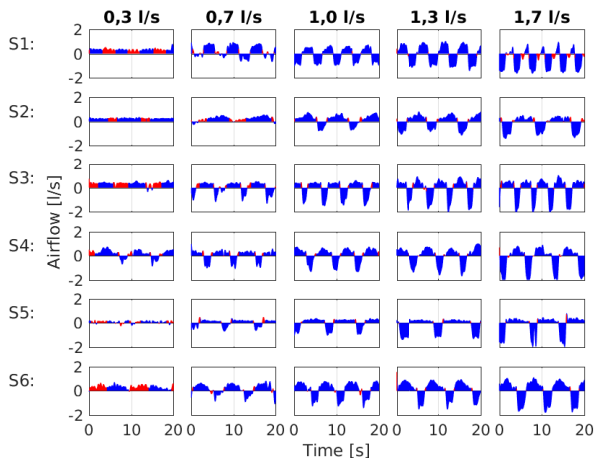


**Fig. 4.** Breathing phase detection (BPD) illustrated with the acoustic airflow estimation waveform for all test subjects (S1-S6), from shallow to deep breathing. Legend: — True BPD; — False BPD

#### 4. DISCUSSION

In Section 3.1.1, we investigate the influence of the selected sensors. The sensor set {2,3} uses only bronchial sounds and the sensor set {9,12} only vesicular lung sounds. Both sensor sets, {2,9} and {3,12}, use bronchial and vesicular lung sounds limited to one hemithorax, respectively. According to Table 1, we obtain the best results with the sensor set {2,3,9,12}. The sensor set over the left hemithorax {3,12} performs poorer than the one over the right hemithorax {2,9}. This might be explained by the stronger contamination with heart sounds on the left side. Figure 3 illustrates the acoustically estimated airflow for the sensor set {2,3,9,12}. In general, we see a good performance for high airflow values during inspiration, unlike for high airflow values during expiration, especially for subjects S1 and S2. This results from the training material, where airflow rate during inspiration is held constant at the given values, while during expiration breathing is natural (cf. Section 2.2). The poor performance for low airflow values results from the low signal-to-noise ratio of the corresponding lung sound recordings.

We investigate the performance of the AAE method performing training and testing on data of the same subject in Section 3.1.2.

This can be seen as a calibration step. In Table 2, we observe small MSE-values, distinctly smaller than in Table 1, i.e. the intro-subject evaluation. The high MSE-value for the recordings with a maximum inspiratory airflow value of 0.3 l/s from subject S1 is due to the contamination of the evaluation material, i.e. the presence of bowel sounds in the lung sound recording of sensor 9.

From the results in Table 3, no substantial differences between the three setups are observable. By high-pass filtering the lung sound (Setup 2), we lose the range with the highest signal-to-noise ratio, because of signal power decrease with increasing frequency [10].

The results in Table 4 show a high accuracy regarding the breathing phase detection for high airflow values. We see that the values for the specificity are close to 100 %, whereas the values for the sensitivity are distinctly lower. According to Figure 4, the relatively low sensitivity at higher airflow values is caused by the false detection of the beginning and/or the end of the inspiratory phase (red areas). As already discussed above, the poor performance at low airflow rates is caused by the low signal-to-noise ratio of the lung sound recordings. A benefit of our acoustic airflow estimation method is its frame-wise breathing phase detection, where no information from previous frames and/or the information about the first phase is needed. This makes the detection robust against swallowing, apnea and coughing, meaning that only the contaminated frames are detected incorrectly.

The limitations of our experiments are the small number of subjects and the lack of metadata, such as age, body height, body weight, gender, etc. Furthermore, we cannot guarantee the accuracy of the recorded airflow signal, because of possible distortions caused by the subjects, i.e. if the tongue is not placed beneath the mouthpiece of the pneumotachograph, the least flow-resistance is not provided. Furthermore, due to the fixed arrangement of the sensors the recording positions vary slightly, because of the different physiques of the subjects.

We can summarize the benefits of the proposed method as follows: We only need one model for acoustic airflow estimation, independent of the breathing phase. It further facilitates a frame-based breathing phase detection. These features make the estimation real-time capable.

#### 5. CONCLUSION

In this paper, we introduce multivariate polynomial regression to acoustic airflow estimation. Therefore, we map spectral features from lung sounds of several recording positions to the airflow values. We evaluate the regression model using mean squared error between estimated and actual airflow and report its accuracy regarding a frame-based breathing phase detection.

Earlier studies for acoustical airflow estimation require calibration, do not use multichannel information of lung sounds and some studies ignored the effect of heart sounds. The proposed method does not need calibration and enables a frame-based breathing phase detection. In experiments, we show good results regarding the acoustic airflow estimation and the breathing phase detection, for high airflow values, even for intro-subject tests. Further experiments indicate no significant impact of heart sounds on the performance of the proposed method regarding acoustic airflow estimation.

Acoustic airflow estimation makes multichannel lung sounds recording/analysis more attractive with respect to medical use, because it renders the pneumotachograph dispensable. Because our experiments are limited to a small number of subjects with a certain physique, as future work, we are planning to evaluate the proposed method on a bigger population from data collected within a clinical trial, and to consider also metadata for the regression model.

## 6. REFERENCES

- [1] S. Huq and Z. Moussavi, "Automatic breath phase detection using only tracheal sounds," in *Proceedings of the 32nd Annual International Conference of the IEEE Engineering in Medicine and Biology Society (EMBC'10)*. IEEE, 2010, pp. 272–275.
- [2] Z. Moussavi, M. T. Leopando, H. Pasterkamp, and G. Rempel, "Computerised acoustical respiratory phase detection without airflow measurement," *Medical and Biological Engineering and Computing*, vol. 38, no. 2, pp. 198–203, 2000.
- [3] A. Yadollahi and Z. Moussavi, "A robust method for estimating respiratory flow using tracheal sounds entropy," *IEEE Transactions on Biomedical Engineering*, vol. 53, no. 4, pp. 662–668, 2006.
- [4] K. Ciftci and Y. P. Kahya, "Respiratory airflow estimation by time varying autoregressive modeling," in *Proceedings of the 30th Annual International Conference of the IEEE Engineering in Medicine and Biology Society (EMBC'08)*. IEEE, 2008, pp. 347–350.
- [5] A. Yadollahi and Z. Moussavi, "Acoustical respiratory flow," *IEEE Engineering in Medicine and Biology Magazine*, vol. 1, no. 26, pp. 56–61, 2007.
- [6] E. Messner, M. Hagmüller, P. Swatek, and F. Pernkopf, "A robust multichannel lung sound recording device," in *Proceedings of the 9th Annual International Conference on Biomedical Electronics and Devices (BIODEVICES'16)*, 2016.
- [7] R. Murphy, "Development of acoustic instruments for diagnosis and management of medical conditions," *Engineering in Medicine and Biology Magazine, IEEE*, vol. 26, no. 1, pp. 16–19, 2007.
- [8] I. Sen and Y. P. Kahya, "A multi-channel device for respiratory sound data acquisition and transient detection," in *Proceedings of the 27th Annual International Conference of the IEEE Engineering in Medicine and Biology Society (EMBS'05)*, 2005, pp. 6658–6661.
- [9] H. Pasterkamp, S. S. Kraman, P. D. DeFrain, and G. R. Wodicka, "Measurement of respiratory acoustical signals. Comparison of sensors.," *CHEST Journal*, vol. 104, no. 5, pp. 1518–1525, 1993.
- [10] A. R. A. Sovijarvi, L. P. Malmberg, G. Charbonneau, J. Vanderschoot, F. Dalmaso, C. Sacco, M. Rossi, and J. E. Earis, "Characteristics of breath sounds and adventitious respiratory sounds," *European Respiratory Review*, vol. 10, no. 77, pp. 591–596, 2000.